Novel Anode Baking Furnace Design for Improved Pit Temperature Uniformity and Anode Quality

Li Han[1], Yanfang Zhang[2], Yingtao Luo[3], Ziwei Su[4], Xiangyu Cang[5], Yujie Wang[6] and Qiaoyun Liu[7]
1. Senior Engineer
2, 3, 4. Professor Level Senior Engineers
5. Assistant Engineer
6, 7. Engineers
Zhengzhou Non-ferrous Metals Research Institute of Chalco (ZRI), Zhengzhou, China
Corresponding author: yanfang_zhang@chinalco.com.cn
https://doi.org/10.71659/icsoba2025-el015

Abstract

With respect to the problems of large temperature differences between the upstream and downstream of the flues and uneven temperature distribution in the pits of traditional flue structure baking furnaces, this study proposes a new flue structure baking furnace. A comparative analysis of temperature distribution uniformity in the pits between traditional flue structure baking furnace and new flue structure anode baking furnace conducted through numerical modelling using CFD software demonstrated that the new baking furnace achieved more uniform temperature distribution in the pit. Test data from an industrial test of the new baking furnace conducted at a carbon plant in Baotou revealed significant improvements in temperature uniformity in the pit of the new structure baking furnace where the average electrical resistivity of calcined anodes decreased by 2.26 μΩ·m, establishing essential conditions for upgrading and enhancing efficiency in aluminium electrolysis production.

Keywords: New baking furnace, Numerical modelling, Anode quality.

1. Background

Carbon anodes in aluminium electrolysis, with the physical and chemical properties (electrical resistivity, bulk density, air permeability, CO_2 reactivity, air oxidation reactivity, mechanical strength, and thermal shock resistance) directly affecting the energy efficiency and operational stability of the electrolytic cell, are the core materials in smelting process. At present, the main open-type ring anode baking furnaces in China are largely based on the improvements of NLM Technology. With respect to the problems of large temperature differences between the upstream and downstream of the flues and uneven temperature distribution in the pits of traditional flue structure baking furnaces, although some companies have attempted to improve quality by adjusting baking curves or optimizing the thermal conductivity of fillers, limited by the fixed layout of the baffle wall of the traditional flue, there is a lack of revolutionary and viable optimization plans. In recent years, foreign researchers have conducted extensive studies and industrial tests on non-traditional (baffle wall-free) flue structure baking furnaces [1, 2], while domestic research on new baking furnaces and anode quality enhancement remains in its infancy [3–6].

Commercial software Fluent was used in this study to investigate and analyse natural gas combustion, flue gas flow, and temperature distribution in baking furnace. A new flue structure baking furnace was developed, and an industrial contrast test was conducted. The results of the industrial test show that the temperature uniformity of the new structure baking furnace has been significantly improved and the electrical resistivity of anodes in the test pit has decreased,

providing a new optimization solution for enhancing the anode quality of the carbon baking furnace.

2. Model Study

2.1 Object of Study and Physical Model

Taking a carbon plant in Baotou as the object of study, the computational domain comprises the representative part between the flue centreline and pit centreline, including flue walls. A schematic diagram of the baking furnace flue (traditional baking furnace) was established as shown in Figure 1.

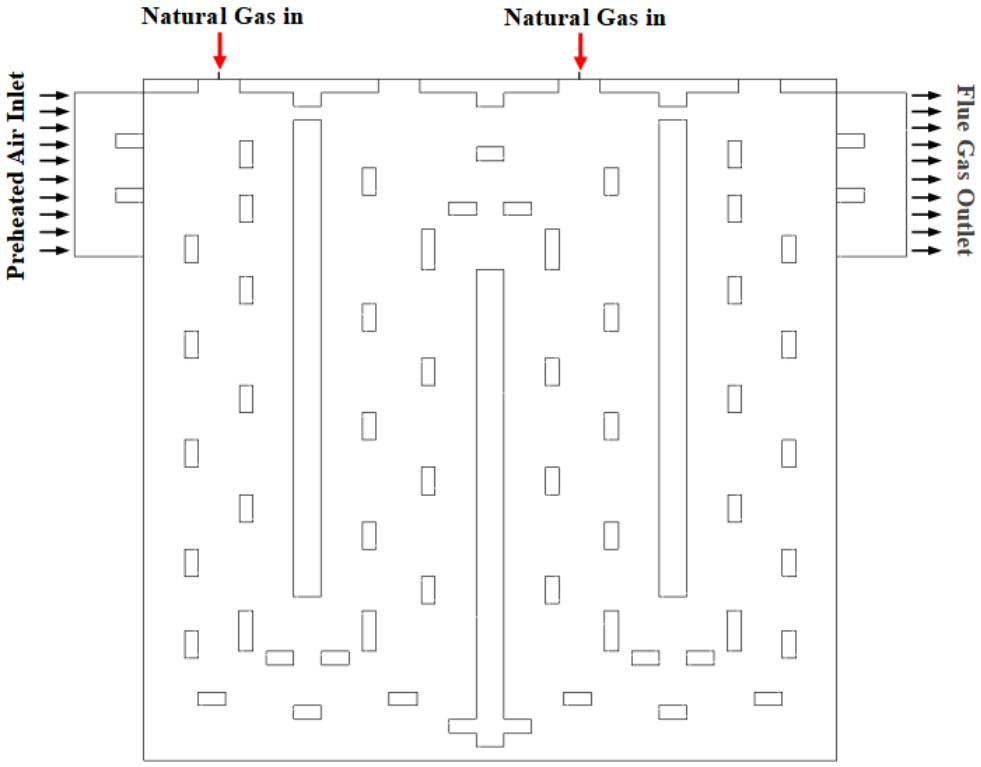

Figure 1. Schematic diagram of model structure and gas in/out.

2.2 Model Assumptions

The study focuses on the thermal performance inside the baking furnace under stable operating conditions of the baking furnace. To enhance computational efficiency of simulation and ensure accuracy of calculation results required for engineering, the following assumptions were made for the physical model:

1) Three layers of green blocks (21 closely connected vertical anode blocks) in the pit are considered as an integral anode block, regardless of gaps and fillers between individual anode blocks;

2) The inlet velocity and outlet pressure are uniform. The flue gas temperature at the inlet of the flue is the average value of the flue gas temperature at the outlet of the previous section;

3) Air infiltration due to negative pressure is disregarded. The combustion of a small amount of volatile passing through the flue walls in the section during high-temperature combustion stage is disregarded;

4) The influence of internal heat source changes caused by chemical reactions within the green block and fillers is disregarded; that is, except for the combustion reaction between natural gas and oxygen, no chemical reactions occur among other substances.

2.3 Mathematical Model

The mathematical model provides a comprehensive description of key processes in the anode baking furnace. The governing equations for each key process form a governing equation system by which the parameters representing the key processes are obtained to identify the information field across the entire interaction space, which are the governing equations describing key processes in the baking furnace in a comprehensive manner. The flow, combustion and heat transfer processes of natural gas in the baking furnace are described by using the system of basic equations for gas combustion.

1) Continuity equation

$$\nabla \cdot (\rho v) = 0 \tag{1}$$

where:

ρ indicates flue gas density in the flue, kg/m^3

v indicates flue gas velocity in the flue, m/s

2) Momentum equation

$$\frac{\partial (\rho v)}{\partial t} + \rho(v \cdot \nabla)v = -\nabla p' + \nabla \cdot (\mu \nabla v) + \nabla \cdot (\mu \cdot (\nabla v)) \tag{2}$$

$$p' = p + (\frac{2}{3}\mu - \xi)\nabla \cdot v$$

$$\mu_{eff} = \mu + \mu_t$$

where:

p' indicates calibrated pressure, Pa

p indicates static pressure, Pa

ξ indicates bulk viscosity

μ_{eff} indicates effective viscosity, kg/m·s

μ indicates laminar viscosity, kg/m·s

μ_t indicates turbulence viscosity.

In the model $k-\varepsilon$, the turbulence viscosity is $\mu_t = C_\mu \rho k^2/\varepsilon$, C_μ=0.09, kg/m·s

3) Energy equation

Gas domain energy equation:

$$\nabla \cdot \left(\rho v \left(h + \frac{v^2}{2}\right)\right) = \nabla \cdot \left(k_{eff} \nabla T - \sum_j h_j \vec{J}_j + \left(\bar{\bar{\tau}}_{eff} \cdot \vec{v}\right)\right) + S_h \tag{3}$$

$$h = \sum_j Y_j h_j$$

$$h_j = \int_{T_{ref}}^{T} C_{p,j}\, dT$$

where:

k_{eff} indicates effective thermal conductivity, $k_{eff} = k_t + k$, W/m·K

k_t indicates turbulence thermal conductivity, calculated based on the turbulence model, W/m·K

$\vec{J}_j$ indicates diffusion flux of component$j$, mol /(m²·s)

S_h indicates source terms, including chemical reaction source term and radiation source term

h_j indicates sensible enthalpy of component$j$, kJ/kg

Y_j indicates mass fraction of component j, %

T_{ref} indicates reference temperature, K

∇T indicates difference between the flue gas temperature and the reference temperature, K

The energy equation of the solid domain (anode and flue wall) is:

$$\frac{\partial}{\partial t}(\rho h) = \nabla \cdot (k \nabla T) \tag{4}$$

where:

h indicates sensible enthalpy, $\int_{T_{ref}}^{T} c_p\, dT$

k indicates thermal conductivity, W/m·K

T_{ref} indicates reference temperature, K

4) Turbulence equation

Turbulence model adopts a standard k-ε model, and the turbulence closure equation k and equation ε are as follows:

$$\nabla(\rho v k) = \nabla\left[\left(\mu + \frac{\mu_t}{\sigma_k}\right) \cdot \nabla k\right] + G_k - \rho\varepsilon \tag{5}$$

$$\nabla(\rho v k) = \nabla\left[\left(\mu + \frac{\mu_t}{\sigma_\varepsilon}\right) \cdot \nabla \varepsilon\right] + C_{1\varepsilon}\frac{\varepsilon}{k} G_k - C_{2\varepsilon}\rho\frac{\varepsilon^2}{k} \tag{6}$$

where:

k indicates turbulence kinetic energy, m²/s²

ε indicates turbulence dissipation rate, the rate at which turbulence kinetic energy is converted into molecular thermal kinetic energy, with no generic unit

$C_{1\varepsilon}$, $C_{2\varepsilon}$, σ_k, σ_ε are the constants in the turbulence model, $C_{1\varepsilon}$ =1.44, $C_{2\varepsilon}$=1.92, σ_k=1.0, σ_ε=1.3

G_k indicates turbulence kinetic energy caused by the average velocity gradient.

5) Combustion equation

Assuming the combustion process is a single-step irreversible reaction under isotropic conditions in chemical equilibrium, the combustion component transport equations describe the variation laws of the mass fractions of chemical components such as fuel, oxidant and products with time and space. For the i chemical component, the transport equation for the mass fraction Y_i is:

$$\nabla \cdot (\rho \vec{v} Y_i) = \nabla \cdot (\rho D_i \nabla Y_i) + R_i + S_i \tag{7}$$

where:

$\nabla \cdot (\rho v Y_i)$ indicates the component variation caused by flow
$\nabla \cdot (\rho D_i \nabla Y_i)$ indicates molecular diffusion caused by concentration gradient, where D_i indicates the component diffusion coefficient, m^2/s
R_i indicates the net production rate caused by chemical reactions
S_i indicates the production rate of user-defined source terms

6) Radiation model
The radiation model adopts the P-1 model, and $-\nabla q_r$ is considered as the heat source (or sink) caused by thermal radiation.

$$-\nabla q_r = aG - 4an^2\sigma T^4 \tag{8}$$

Radiation flux q_r:

$$q_r = -\frac{1}{3(a+\sigma_s)-C\sigma_s}\nabla G \tag{9}$$

where:
a indicates absorption coefficient, 1/m
σ_s indicates scattering coefficient, 1/m
G indicates incident radiation, W/m^2
C indicates linear-anisotropic phase function coefficient,
n indicates refractive index of the medium, dimensionless
σ indicates Boltzmann constant, 1.38×10^{-23} J/K

3. Analysis of Computing Results

By conducting simulation calculations using the same boundary conditions and mathematical models as traditional baking furnaces, based on the optimization objectives and factors analysed in the study, an optimized new flue structure plan was obtained. The trend of flue gas flow in the flue is shown in Figure 2. The right panel shows the first version of the new baking furnace structure, where after the removal of the baffle walls, the trend of flue gas flow in the flue has changed significantly. The temperature distribution in the pit is shown in Figure 3. The right panel shows the corresponding temperature distribution in the baking furnace pit after multiple optimizations.

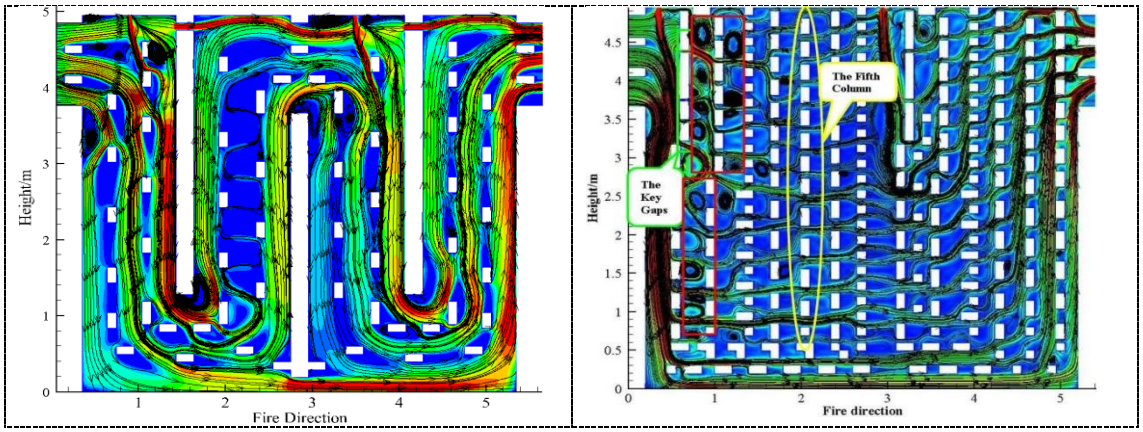

Figure 2. Flue gas flow in baking furnace flue. Left: traditional structure; Right: new structure.

From the comparison diagrams of Figures 2 and 3, it can be seen that the traditional baking furnace flue features three baffle walls, resulting in "W"-shaped distribution of flue gas flow in the flue, extending flow time of high-temperature flue gas in the flue and enhancing heat transfer between the high-temperature flue gas and pits. However, the only channel for flue gas causes a large

pressure loss in the flue and a large temperature difference between the upstream and downstream. The baffle walls in the new anode baking furnace flues have been removed and laying of the bricks have been rearranged. The high-velocity flue gas flows in a "U"-shaped outer ring, while the low-velocity flue gas flows horizontally in the middle of the flue. The flue gas flow channels are not unique and there is no obvious upstream and downstream distinction, reducing the overall temperature difference in the pit. In addition, by optimizing the reasonable gaps between the bricks, on the one hand, the flue gas volume escaping along the shortest path is reasonably controlled, and on the other hand, the relative high temperature in the local small vortex area is maintained to increase the overall temperature in the pit.

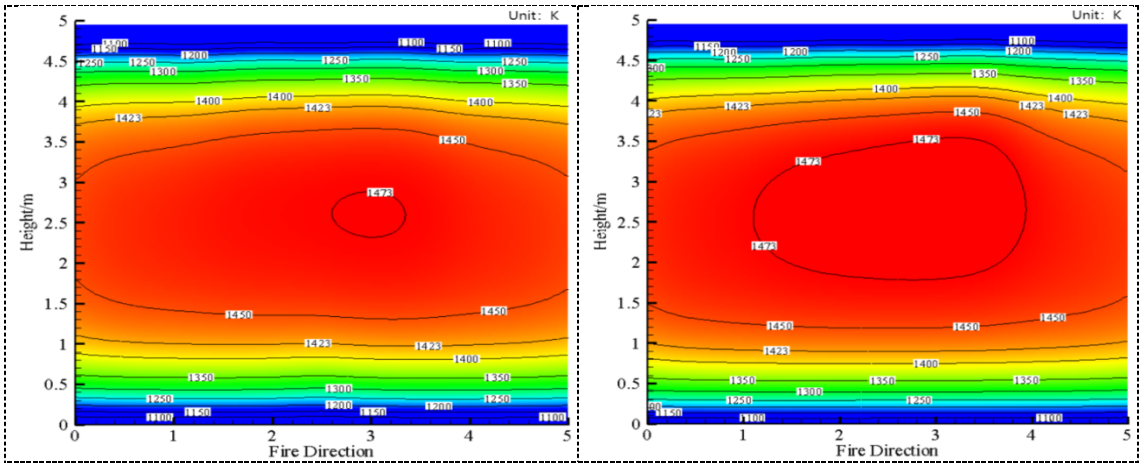

Figure 3. Temperature distribution in baking furnace pit. Left: traditional structure; Right: new baking furnace.

To quantitatively analyse the uniformity of temperature distribution in the pits of traditional baking furnaces and new baking furnaces, equidistant points at the positions of calcined anode blocks in the pits were selected to acquire and analyse temperature data at the points (marked with "+") and the standard deviation of the equidistant point temperature data was used to evaluate the uniformity of temperature distribution. The standard deviation can accurately reflect the dispersion of the equidistant point temperature data relative to the mean value: a smaller standard deviation indicates gentler temperature variations and a better temperature uniformity, while a larger standard deviation indicates greater temperature variations and uneven temperature distribution. Through this approach, influence of temperature on the quality of anode baking was assessed.

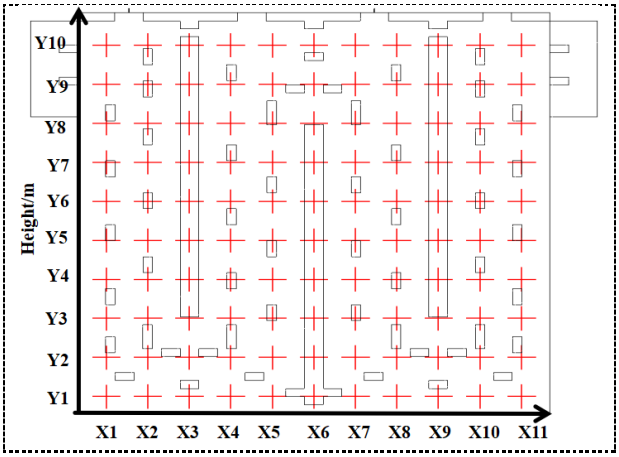

Figure 4. Schematic diagram of equidistant point distribution on the centre plane of the pit.

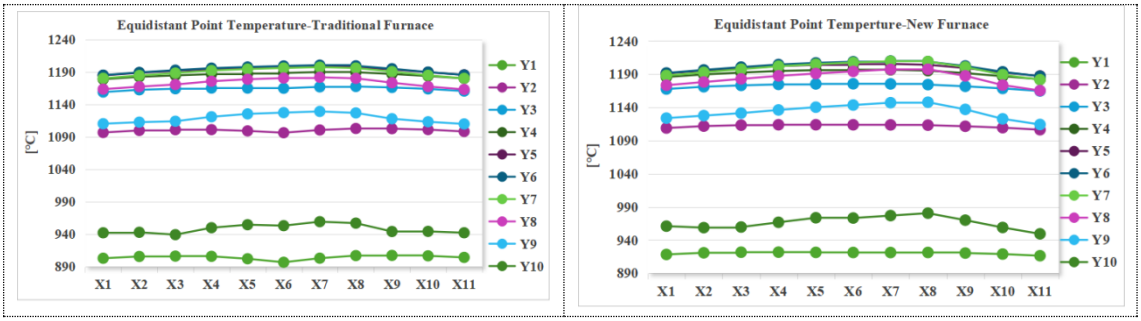

Figure 5. Trend of temperature data at equidistant points in the pits. Left: traditional structure; Right: new structure.

Table 1. Key data at equidistant points.

	Traditional Furnace	New Furnace
Average temperature (℃)	1117.37	1127.43
Standard deviation (℃)	117.1	95.3
Maximum difference (℃)	313.9	281.6
External wall ($W/m^2 \cdot K$)	12.03	13.27
Pressure loss（Pa）	20.26	19.01

Through comparative analysis of the temperature distribution trend and data at equidistant points, it can be seen that:

1) The highest temperature points in the pits of traditional flue and new flue correspond to the heights along the flame direction (X4–X8). The lowest temperature point in the pit of traditional flue is located at (X6, Y1), the highest temperature point is located at (X7, Y6), with the maximum temperature difference of 313.9 ℃; the lowest temperature point in the pit of new flue is located at (X4, Y10), with the maximum temperature difference of 281.6 ℃; the temperature range in the pit of new flue is 32.3 ℃ smaller than that of the traditional structure;

2) The overall temperature distribution in the pit of traditional flue is extremely uneven, with a temperature standard deviation of 117.1 ℃. The temperature standard deviation in the new structure pit is 21.8 ℃ lower than that of the traditional structure, with smaller temperature fluctuations and significantly improved temperature distribution uniformity.

4. Comparative Analysis of Industrial Test Results

Based on optimized new flue structure calculated through simulation, engineering design of the baking furnace structure and retrofitting of the flues were carried out and an industrial test for one production cycle was also conducted.

4.1 Equivalent Temperature Analysis

The baking degree of the baking furnace was measured using equivalent temperature. Corundum crucibles were placed at test positions as shown in Figure 6. From the positions where corundum crucibles were placed for equivalent temperature test, calculated results corresponding to the positions were acquired for comparative analysis. In addition, the temperature data from two pits at a carbon plant in Shanxi and two pits at a carbon plant in Chibi was tested as shown in Figures 7 and 8. The test data of the traditional structure pit and new structure pit at the carbon plant in Baotou is shown in Figures 9 and 10.

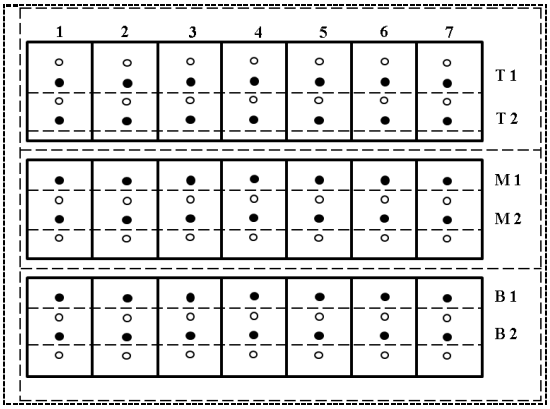

Figure 6. Distribution of crucibles for equivalent temperature testing.

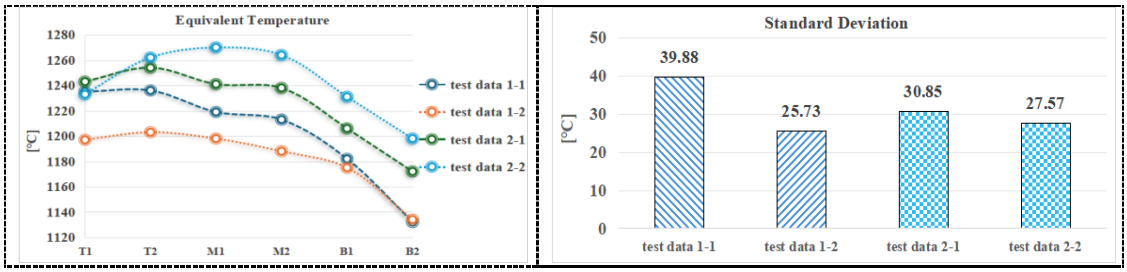

Figure 7. Test data from two pits at two plants. Left: equivalent temperature distribution trend; Right: standard deviation.

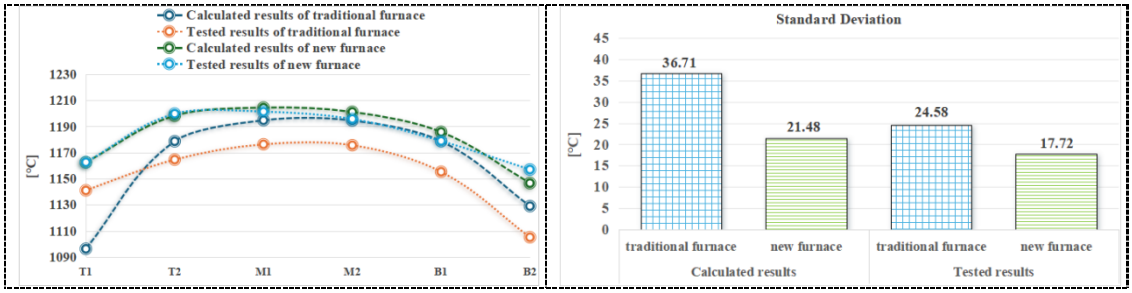

Figure 8. Equivalent temperature data of test pit and new pit. Left: equivalent temperature distribution trend; Right: standard deviation.

From Figure 7, it can be seen that:

1) In traditional structure baking furnaces, due to the single-channel flow of flue gas and escape of high-temperature flue gas through upper fire holes along the shortest path, the baking temperature of the upper layer of carbon blocks in the baking furnaces is relatively high, while that of the lower layer of carbon blocks is relatively low.

2) Standard deviation of the temperature in the pits of the traditional structure baking furnaces is above 25 ℃. The maximum standard deviation is 39.88 ℃, and the minimum standard deviation is 25.73 ℃.

From Figure 8, it can be seen that:

1) The distribution of the tested results of the average temperature of the equivalent temperature of each carbon block is consistent with the trend of the calculated results. Due to the certain hypothetical nature of the computational model, the tested results are slightly

lower than the calculated results, and the temperature in the pit of new baking furnace is slightly higher than that of the traditional baking furnace.

2) The temperature standard deviation trend of all test points of the test results are consistent with that of the calculated results. The uniformity of temperature distribution in the pit of the new baking furnace is better than that of the traditional baking furnace. Based on the calculated results, the temperature uniformity of the new baking furnace pit is 15.2 ℃ better than that of the traditional baking furnace; based on the tested results, the temperature uniformity of the new baking furnace pit is 7.8 ℃ better than that of the traditional baking furnace, with a smaller fluctuation in the equivalent temperature distribution, demonstrating that the temperature distribution in the new baking furnace is more uniform, and the temperature uniformity has been improved and enhanced to a certain extent compared with the traditional structure pit.

4.2 Anode Quality

In order to further verify the baking effect of the new baking furnace, samples were taken from the anodes in the test pit and the control pit, and the physical and chemical indicators of the samples were analysed. The average data of the indicators are shown in Table 2.

Table 2. Parameters of physical and chemical indicators of calcined anodes.

Parameter	True Density (g/cm^3)	Electrical Resistivity ($\mu\Omega \cdot m$)	Flexural Strength (MPa)	Air Permeability (nPm)
New Furnace	1.582	56.54	10.4	1.89
Traditional Furnace	1.575	58.8	8.5	2.9

It can be seen from Table 2 that the density of the calcined anodes in the new anode baking furnace increased by 7 kg/m^3, the average electrical resistivity decreased by 2.26 $\mu\Omega \cdot m$, the air permeability decreased by 1.01 nPm, and the bending strength increased by 1.9 MPa, demonstrating that the quality and performance of the anodes have been improved and enhanced to a certain extent.

5. Conclusion

The flow in the flue and the temperature uniformity in the pit of the anode baking furnace were investigated via CFD software. The high-temperature flue gas flow in the new baking furnace is mainly horizontal, with relatively uniform flow field distribution, reducing the temperature difference between the upstream and downstream. The standard deviation (temperature uniformity) in the new baking furnace pit is better than that in the traditional baking furnace pit.

The industrial test results show that the trend of the tested results is consistent with that of the calculated results. The temperature uniformity in the pit of the new anode baking furnace is superior to that of the traditional baking furnace, with the average electrical resistivity decrease of 2.26 $\mu\Omega \cdot m$, and the bulk density increase of 7 kg/m^3, demonstrating that the quality and performance of the calcined anodes have been improved and enhanced.

Currently, the new baking furnace has being subject to industrial tests at a carbon plant in Qinghai with respect to additional flues, multiple cycles and multiple parameters.

6. References

1. Dagoberto Schubert Severo et al., Recent developments in anode baking furnace design, *Light Metals* 2011, 853–858. https://doi.org/10.1007/978-3-319-48160-9_146
2. Magali Gendre, A breakthrough in anode baking furnace flue-wall design, *Light Metals* 2007, 969–972.
3. Yingtao Luo, et al., *A flue structure of carbon baking furnace*, CN 108826990A, Applied on May 9, 2018, Authorized on October 25, 2019 (in Chinese).
4. Yingtao Luo, et al., Flue Structure. CN 114508938B, Applied on January 14, 2022, Authorized on January 24, 2024 (in Chinese).
5. Li Han, Yanfang Zhang, Yingtao Luo. Numerical simulation analysis and research on the new flue structure anode baking furnace, *Light Metals,* 2022, 45–49 (in Chinese).
6. Li Han, et al., Simulation energy-saving analysis and application of new anode baking furnace, *Light Metals,* 2025, 996–1003. https://doi.org/10.1007/978-3-031-80676-6_124